Journal of University of Babylon, Engineering Sciences, Vol.(26), No.(5): 2018.

Experimental and Theoretical Investigation of Impinging Jet Ventilation at Different Cross Sectional Area of Supply Air Duct

Ala'a Abbas Mahdi **Sara Mohammed Abbas**
Department of Mechanical Engineering, College of Engineering, Babylon University
alaa.mahdi1959@gmail.com alifahem1988@gmail.com

Abstract

An experimental and computational analysis of temperature and velocity distribution in an office room have been studied. Office room of dimensions (3m x 1.75m x 3m) with two cross sectional types of supply air duct in the experimental part and three different cross sectional types of supply air duct in the theoretical part is usual as a tested model. The RNG k-ε turbulence model was employed to solve the governing equations numerically and validated by comparing the numerical results with experimental data. The impinging jet concept has been proposed as a new ventilation strategy for use in office and industrial buildings. The present work focuses on evaluating the performance of a new impinging jet ventilation. In a theoretical study three types of supply air duct are adopted which are square supply air duct (Type-I), semi-elliptic supply air duct (Type-II) and rectangle supply air duct (Type-III) for two cases of air outlet terminal height from room foot level, 0.14h (case-I) & 0.1h (case-II). The third type (rectangle duct) gives lowest effective and discomfort conditions when compared with the other two types. This study investigated a number of factors influencing draught discomfort and temperature stratification in an office environment equipped with impinging jet ventilation IJV. The factors considered to be: shape of the air supply device, supply airflow rate and supply air temperature. Acceptable Air Distribution Performance Index (ADPI), effective temperature, and ventilation efficiency obtained that the square cross sectional area of supply air duct at 0.1h (case-II) height from foot level gives more acceptable indoor air quality and human thermal comfort when compared with the other types. Also, this type gives good air distribution system not only promotes a comfortable and healthy environment for occupants, but also contributes to energy conservation.

Keyword: - Impinging jet ventilation, CFD, Measurement, Indoor air quality, Turbulence model, wall jet.

الخلاصة

يتضمن البحث دراسة عملية ونظرية لحركة الهواء وتوزيع درجة الحرارة داخل حيز باستحدام منظومة تهوية البثق المؤثر لغرفة مكتب واستخدام برامج الحاسوب (ANSYS.١٥) لحل معادلاث نافير ستوك باستخدام طريقة الفروقات المحددة لمحاكاة وتحليل النموذج المدروس . تم اختبار ثلاثة انواع لمجاري دفع الهواء تم استحدام مجرى هواء مقطع مربع ونصف دائري ومستطيل الشكل بارتفاع(٠,١٤h,٠,١h) عن مستوى الارض تم قورنت النتائج النظرية مع القراءات العملية حبث تم التواصل الى ان المقطع المربع هو النوع الاكثر مقبولية بين الانواع الثلاثة الاخرى في الحالة المدروسة بالنسبة لراحة الشاغلين

الكلمات المفتاحية:- منضومة تهوية البثق، ديناميك الموائع البرامجي او الحاسوبي، قياسات، نوعية الهواء الداخلي، الموديل الاضطرابي، بثق جداري.

Nomenclature

Symbols	Description	Unit
A_f	Surface area for floor	m^2
A_s	Face area for diffuser	
C_p	Specific heat of the air at constant pressure.	kJ/kg.K
dx dy dz	Control volume	m
E_{ij}	The mean rate of deformation tenser	
g	Gravitational acceleration	m/s^2
$k_{i,j,k}$	Turbulent kinetic energy at cell (i,j,k)	m^2/s^2
P	Pressure	N/ m²
P_z	zone population	person
Q_{DV}	Air required to satisfy the sensible cooling load in a DV system	l/s
q_l	Cooling load for the overhead lighting	W
q_{oe}	Cooling load for occupants, desk lamps and equipment.	W
Q_{oz}	Fresh air flow rate	l/s
R_A	Outdoor air flow rate required per unit area	l/s
R_p	Outdoor air flow rate required per person	l/s
S	Source term for the rate of thermal energy production	J/kg
T_{av}	average room temperature	^oC
$T_{i,j,k}$	Temperature at cell (i,j,k)	^oC
ΔT_{hf}	Temperature difference from head to foot level.	^oC
T_{sp}	Setup (design) temperature.	^oC
U_s	Supply air velocity	m/s
U_x	Local air velocity	m/s

Abbreviations

ASHRAE	American Society for Heating Refrigeration and Air Conditioning Engineering		
ACH	Air change per hour		
CFD	Computational Fluid Dynamics		
DV	Impinging Ventilation		
IAQ	Indoor air quality		
RNG	Re-Normalization Group		
IJV	Impinging Jet Ventilation		
MV	mixing ventilation		
DV	displacement ventilation		
Sub-Scripts			
av.	Average	sp	Setup
f	Floor	t	total
l	Overhead light		
Greek letters			
ρ	Air density	kg/m^3	
Ɛ	Turbulent energy dissipation rate.		

σ	Prandtl or Schmidt number	
ω	specific dissipation rate	1/s
Γ	Diffusion coefficient (diffusivity)	m^2/s

1- Introduction

A new method of air distribution known as the Impinging Jet Ventilation (IJV), this method based on the principle of supplying a jet of air with high momentum downwards onto the floor. As the jet impinges onto the floor it spreads over a large area, causing the jet momentum to recede, but still has a sufficient force to reach long distances (Karimipanah[a], 2001).

The quality of the indoor environment is of significance to the occupants' health, comfort and productivity, as nowadays people spend most of their time indoors. On the other hand, mechanical ventilation systems use large amounts of energy in order to achieve the desired indoor environment. This poses great challenges for the design of ventilation systems, not only to provide a healthy environment, but also to achieve efficient use of energy. To fulfil such requirements, a new type of ventilation system, termed impinging jet ventilation (IJV), for use in office environments, classrooms and industrial premises (Karimipanah, 2002; Chen, 2013; Rohdin, 2007).

For impinging jet ventilation system, there are only a few studies available in the literature. It was found that the discharge height has a slight influence on the maximum jet velocity decay (Karimipanah, 2002; Chen, 2012; Varodoumpun, 2007) and temperature pattern (Varodoumpun, 2007), but the effect on thermal comfort and IAQ is more than anticipated (Varodompun, 2007; Chen, 2012)studied the shape of the supply device under isothermal conditions, and it was revealed that the supply diffuser configuration plays a significant role in determining the flow pattern over the floor. Other parameters such as heat load and air supply outlet area have also been investigated (Varodompun, 2007). Based on the findings from the literature and the authors' previous studies, the parameters of both configuration and supply flow of impinging jet systems will be the focus of this study, and the subsequent effects will be mainly evaluated with respect to the draught discomfort and temperature gradient, which are the issues of most concern for impinging jet ventilation.

To avoid local thermal discomfort risk for such low-level air supply systems, a systematic study on the factors influencing draught sensation and thermal stratification is necessary. Moreover, establishing a correlation between the influencing and performance factors is of great practical importance, which can help ventilation engineer's correctly select optimal parameters at design stage.

Previous research's found that the number of parameters play an important role in the room air diffusion and temperature stratification, which in turn influence thermal comfort and indoor air quality (IAQ).

The supply air temperature and vertical location of air inlets can affect the airflow pattern in the lower part of the room, but not so much in the upper zone (Lee, 2012).

The objective of this study is to investigate the effect of different configurations and flow parameters of impinging jet ventilation (design varies) under Iraqi hot climate, i.e., the shape of the air supply device for at different heights from room foot level, the supply airflow rate and temperature, on local thermal discomfort parameters (response variable), i.e. the temperature difference from the ankle to head level in an office room. The effect on thermal comfort assessed by the index of the predicted mean vote (PMV) within the office room will also be studied.

2- CFD Modeling

2-1 Turbulent Impingement Models

The physical model beneath consideration is a test room provision like two people's offices, with dimensions (3 x 1.75 x 3) m. Various components are used to simulate summer working environment, air flow rate is 34.825 l/s and the air supply temperature is (20.08 ^{o}C), a turbulence intensity of 5% ,i.e. two PC-simulator (90 W), two manikin (80 W), lighting (100 W), heated floors (150 W), The IJ device is installed and the exhaust is opened on the same side wall as shown in Fig. (1).

Indoor air temperature and velocity distribution recorded from the three poles at different levels from room foot level fixed on each pole by adopting the supply air IJV system of the different cross sectional area located vertically at the center of the north wall, and is discharged from a terminal at a different height above the foot level as shown in Figs. (2 to 7). The air distribution performance index (ADPI) is the percentage determined by the number of measured points in an occupied area where it is within the specified limit (> -1.7 ° C and <1.1 ° C) on the total number of points measured, A literature index of between 60 and 69 is unsatisfactory, 70 to 79 satisfactory and 80 and up as a good distribution of air.

When properly selected, most ports can achieve an agreeable ADPI evaluation. The higher the ADPI rate, the greater the quality of air circulation within the room. Generally, literary of 80 is considered agreeable.

Numerical results were adopted in the current study of the chamber tested using many calculations in different aircraft and all fields as illustrated in Fig. (8) And locations presented in table 1.

A solution is defined for flow field problems (temperature, pressure, speed, etc.) in the nodes per cell.

The precision of the CFD solution is governed by the number of cells in the network. Generally the largest number of cells, the best precision of the solution. Fig. (9), show part of the meshed model for supply air duct shape (types-I, II, III) and at a different air outlet height from room foot level (case I-II).

When solving the problem numerically it is impossible to obtain a precise solution, so the residue of the scaling error must be selected acceptable for different expressions such as continuity, speed and power components.

The boundary conditions are defined as follows: The working fluid used is air and the flow assumed to be steady, three-dimensional, incompressible fluid, Newtonian and turbulent flow. The Ansys Fluent15 code software was used to generate the model and meshed case study, depending on many testing meshes then analyses by using Ansys Fluent15 code software until the residual error for solving equations arrived in (10^{-3}) and (10^{-6}) for energy equation. Second-order upwind scheme using for the convection terms. PRESTO (Pressure Staggering Option) scheme is used for the pressure. For the pressure-velocity coupling the SIMPLEC scheme is used. When working with unstructured meshes, a high-order scheme is preferred for the discretization of convection terms to minimize the discretization errors.

Fig. 2. Schematic drawing of the office room, type-I, case-I

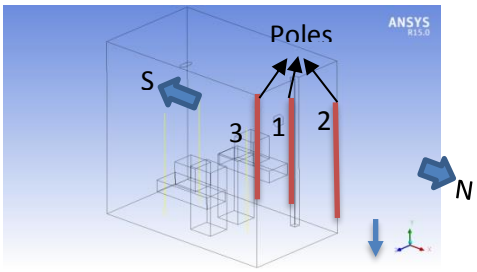

Fig. 1. Configuration of tested room

Fig. 3. Schematic drawing of the office room, type-I, case-II

Fig. 4. Schematic drawing of the office room, type-II, case-I

Fig. 5. Schematic drawing of the office room, type-II, case-II

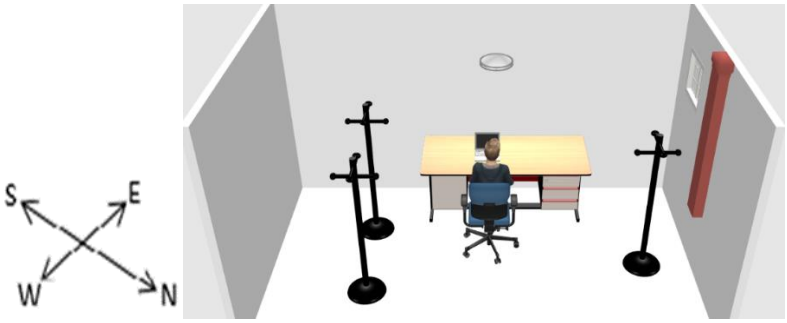

Fig. 6. Schematic drawing of the office room, type-III, case-I

Fig. 7. Schematic drawing of the office room, type-III, case-II

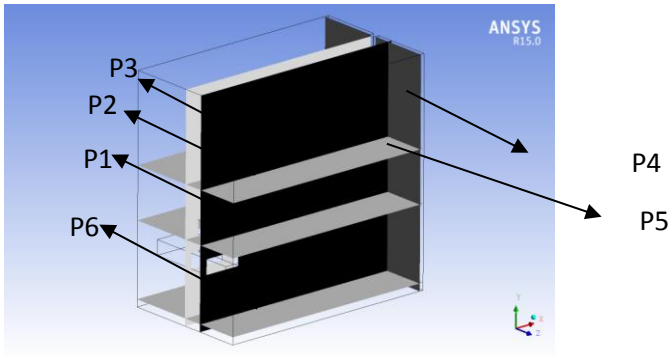

Fig. 8. The schematic geometry of a room is useful for plot plane for all types.

TABLE 1 The planes locations

No.	*Title of plane*	*plane*	*Location m*
1	Plane 1	ZX	Y=1.1
2	Plane 2	ZX	Y=1.8
3	Plane 3	XY	Z=0.875
4	Plane 4	ZY	X=2.95
5	Plane 5	XY	Z=1.15
6	Plane 6	XZ	Y=0.1

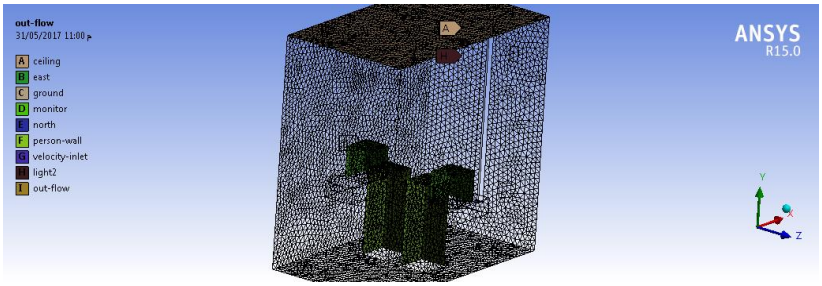

Fig. 9. Mesh configurations with finer gird distributions near wall surfaces Type-I, Case-I

3- Governing equations

The working fluid is air and the flow assumed to be steady, three-dimensional flow, incompressible fluid and Newtonian turbulent flow.

The governing equations of motion based on Navier-Stockes equations, conservation form of continuity, momentum and energy equations as follows (Chen, 2003).

$$\frac{\partial}{\partial x}(\rho u)+\frac{\partial}{\partial y}(\rho v)+\frac{\partial}{\partial z}(\rho w)=0 \tag{1}$$

$$\frac{\partial}{\partial x}(\rho UU)+\frac{\partial}{\partial y}(\rho UV)+\frac{\partial}{\partial z}(\rho UW)=-\frac{\partial p}{\partial x}+\frac{\partial}{\partial x}(\mu\frac{\partial U}{\partial x})+\frac{\partial}{\partial y}(\mu\frac{\partial U}{\partial y})+\frac{\partial}{\partial z}(\mu\frac{\partial U}{\partial z}) \tag{2}$$
$$+\frac{1}{3}\frac{\partial}{\partial x}\left[\mu(\frac{\partial U}{\partial x}+\frac{\partial V}{\partial y}+\frac{\partial W}{\partial z}\right]+\rho g_x$$

$$\frac{\partial}{\partial x}(\rho UV)+\frac{\partial}{\partial y}(\rho VV)+\frac{\partial}{\partial z}(\rho VW)=-\frac{\partial p}{\partial y}+\frac{\partial}{\partial x}(\mu\frac{\partial V}{\partial x})+\frac{\partial}{\partial y}(\mu\frac{\partial V}{\partial y})+\frac{\partial}{\partial z}(\mu\frac{\partial V}{\partial z}) \tag{3}$$
$$+\frac{1}{3}\frac{\partial}{\partial y}\left[\mu(\frac{\partial U}{\partial x}+\frac{\partial V}{\partial y}+\frac{\partial W}{\partial z}\right]+\rho g_y$$

$$\frac{\partial}{\partial x}(\rho UW)+\frac{\partial}{\partial y}(\rho VW)+\frac{\partial}{\partial z}(\rho WW)=-\frac{\partial p}{\partial z}+\frac{\partial}{\partial x}(\mu\frac{\partial W}{\partial x})+\frac{\partial}{\partial y}(\mu\frac{\partial W}{\partial y})+\frac{\partial}{\partial z}(\mu\frac{\partial W}{\partial z})+ \tag{4}$$
$$\frac{1}{3}\frac{\partial}{\partial z}\left[\mu(\frac{\partial U}{\partial x}+\frac{\partial V}{\partial y}+\frac{\partial W}{\partial z}\right]+\rho g_z$$

$$\frac{\partial}{\partial x}(\rho UT)+\frac{\partial}{\partial y}(\rho VT)+\frac{\partial}{\partial z}(\rho WT)=\frac{\partial}{\partial x}\left(\Gamma\frac{\partial T}{\partial x}\right)+\frac{\partial}{\partial y}\left(\Gamma\frac{\partial T}{\partial y}\right)+\frac{\partial}{\partial z}\left(\Gamma\frac{\partial T}{\partial z}\right) \tag{5}$$

3-1 Turbulence models:

RNG K-Ɛ turbulence model is used with the following equations (Chen, 2003):

RNG K-Ɛ model:

$$\rho U_i \frac{\partial k}{\partial x_i} = \mu_t S^2 + \frac{\partial}{\partial x_i}[\alpha_k \mu_{eff} \frac{\partial k}{\partial x_i}] - \rho\varepsilon \quad (6)$$

$$\rho U_i \frac{\partial \varepsilon}{\partial x_i} = C_{1\varepsilon}(\frac{\varepsilon}{k})\mu_t S^2 + \frac{\partial}{\partial x_i}[\alpha_k \mu_{eff} \frac{\partial k}{\partial x_i}] - C_{2\varepsilon}\rho(\frac{\varepsilon^2}{k}) - R \quad (7)$$

The values of model constants are: $C_{1\varepsilon}$=1.42 and $C_{2\varepsilon}$=1.68.

4- Experimental Work

4-1 Tested room

A set of full-scale office room experiment was conducted to study the airflow, temperature, and transport with the IJV system at a different cross sectional area of the supply air duct. The tested room delivered and setup by all the necessary equipment's for the IJV system as shown in Fig. (10).

4-1-1 Configuration room

Full scale office room experiments was adopted to study temperature distribution and velocity magnitude using IJV system under Iraqi hot climate by using three types of cross sectional area of the supply air duct. The dimensions of test office room area (length x width x height) (3 x 1.75 x 3) m, which is furnished for two person simulator (shape of human body properties represented by using manikin. The assumed elevation of human manikins is 1.1m (breathing zone) for a person at sitting situation, with a heat source of 80W placed inside manikin to generate the amount of heat from human body having the same surface area and releasing heat similar to a human, two PC-simulator, two tables, one lamp were placed as a heat source for different supply air duct as shown in Figs. (11 to 14). The exhaust grille located below the ceiling on the north side wall, one door located on the west side and the cooled air delivered by using an air conditioner unit of cooling capacity of (7.0344kw).

a b

Fig. 10. Photograph of the (a) experimental isothermal tested room (b) air conditioner unit with supply air duct

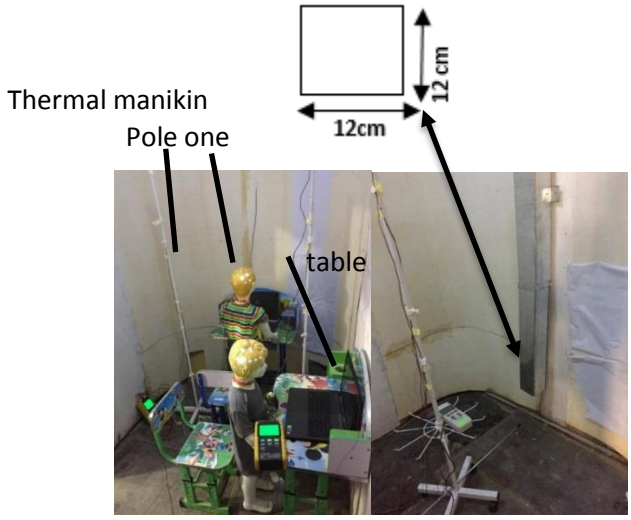

a b

Fig. 11. The layout of the test room for the isothermal (a) The test office room (b) type-I, case-I.

a **b**

Fig. 12. The layout of the test room for the isothermal (a) The test office room (b) type-I, case-II

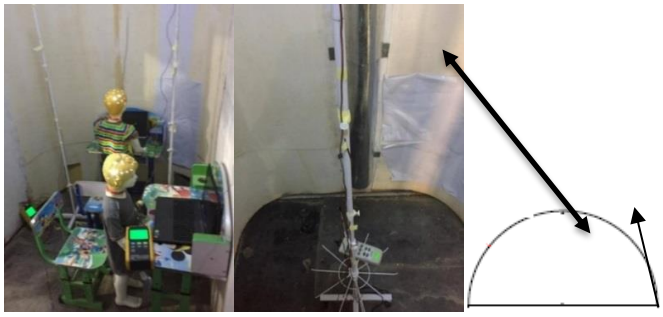

a **b**

Fig. 13. The layout of the test room for the isothermal (a) The test office room (b) type-II, case-I

Fig. 14. The layout of the test room for the isothermal (a) The test office room (b) type-II, case-II

3- Air handling and supply system

There are two steps to find ventilation rate and supply air temperature for ventilation applications. The procedures are based on the findings of ASHRAE research, Project-949.

Step one: Supply flow rate

a- Calculation of the cooling load ventilation air flow rate, Q_{IJV}:

Equation (8) used to calculate the amount of air flow rate air needed for ventilated room (ASHRAE, 2004)

$$Q_{IJV} = (0.295q_{oe}+0.132q_l+0.185q_{ex})/ (\rho\ c_p\ \Delta T_{hf}) \quad (8)$$

All heat transported through walls and windows to the room should be taken into account when calculating the external heat gain (q_{ex}) using the equation (9).

$$Q= U\times A\times (T_o-T_{sp}) \quad (9)$$

$$U= 1/ R_{th} \quad (10)$$

$$R_{th} = \frac{1}{h_i} + \frac{x_1}{k_1} + \ldots\ldots + \frac{x_n}{k_n} + \frac{1}{h_o} \quad (11)$$

b- Calculation of fresh air flow rate, Qoz:

From ASHRAE Standards 62.1-2004 (Chen, 2003) Equation (12) is used to determine the flow rate of fresh air.

$$Q_{oz} = \frac{R_p P_z + R_A A_f}{E_z} \quad (12)$$

The values of (R_p, R_A, P_z and E_z) determined from (ASHRAE standards 62.1-2004; Chen, 2003). Then, choose the largest value of flow rate calculated from (a&b) as the design flow rate of the supply air:

Step two: Supply air temperature:

Equations (13&14) used to determine the supply air temperature (T_s) for displacement ventilation applications (Awbi, 2003).

$$T_s= T_{sp} -\Delta T_{hf} - [(A_f.\ q_t) / (0.584Q_{DV}^2+1.208A_f.Q_{DV})] \quad (13)$$

$$q_t = q_{oe} + q_l \quad (14)$$

Then to determine the air flow rate and supply temperature applied the following values (ASHRAE. Standard 55-2004):

q_{person}	$q_{computer}$	T_{sp}	ΔT_{hf}
75 W	45 W	24 ºC	2 ºC

Values of air flow rate (Q_s) and air supply temperature (T_s) can be obtained and listed in table (5). The air change per hour (ACH) can be calculated by using equation (15) (Awbi, 2003).

$$ACH = (Q_s/V_{Room}) \times 3600 \quad (15)$$

Table (2) Values of air flow rate (Q_s), supply air temperature (T_s) and air change per hour (ACH).

Q_s *(l/s)*	T_s *(ºC)*	*ACH*
34.83	20.08	7.96

3-1 Design of Supply Air Duct

In impinging jet ventilation there are some goals must be investigated the airflow and temperature fields, thermal comfort as well as ventilation effectiveness with respect to heat removal effectiveness and air exchange efficiency of the impinging jet ventilation system for an office environment.

of the three different types of the air supply duct used to present work with different opening height from the foot level. The supply air velocity 2.5m/s, then equation (16) is used to calculate cross sectional area for each air duct, (Huijuan, 2014).

$$Q_s = u_x \times A_s \quad (16)$$

The dimensions of the supply air duct for all types are listed in table (3).

Table (3) Area and length of the two different high velocity air duct

Supply air duct	*Type-I Square air duct*		*Type-II Semi-elliptic Air duct*		*Type-II Rectangle Air duct*	
Cross sectional area m^2	0.0144		0.01393		$8*10^{-3}$	
Duct length	0.14h	0.1h	0.14h	0.1h	0.14h	0.1h
M	2.58	2.7	2.58	2.7	2.58	2.7

4- Experimental Procedures

Measuring of airflow field velocity and temperature distribution were recorded in the test room on three poles. Each pole has six nods being placed at various height levels of (0, 0.4, 0.8, 1.1, 1.4 & 1.8) m from the foot level. The first pole used to record parameters that is located at (x=2, y=0, z=0.875) m from the zero source point. The second pole is located at (x=0.7, y=0, z=0.5) m from the zero source point, and the third pole located at (x=0.7, y=0, z=1.25) m from the zero source point. A sensor measured the temperature at each point of these poles. Also, at pole number one a hot wire device is used to record air velocity in terms of supply air duct and relative humidity at the breathing zone (1.1 m) near the supply air outlet. This device used to check the air velocity at the terminal of supply air duct, which is equal 2.5m/s and recorded the related humidity equal 42%.

To measured air temperature distributions inside the tested room, three vertical poles Fig. (20) Are placed. A twenty four number of thermocouples type K was used to record air temperature. Temperature logger of 12 channels with universal thermocouple

was used in the experimental work. All thermocouples are connected to a computer which is controlled by a data acquisition (BTM-4208SD) to register the value from the thermocouples as shown in Fig. (21).

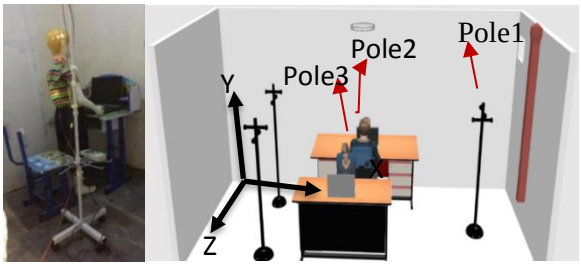

a **b**

Fig (15). Layout of a pole for different measurements

(a) Schematic diagram of pole, (b) Photograph of pole location.

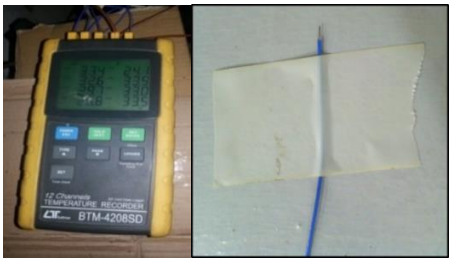

a **b**

Fig (16). Surface temperature measurement system a- Temperature recorder b- Thermocouple attached to wall surfaces

a. **Experimental Readings**

The experimental readings recorded in May (2017) at a steady state time (14:00 p.m.) as listed in tables (4, 5)

Table 4 Experimental results obtained by adopting IJV System, case-I (0.14h)

Type of supply air duct	Pole No.	Thermocouple height from the foot level(m)					
		0	0.4	0.8	1.1	1.4	1.8
		Air temperature (^oC)					
Type-I (square air duct)	Pole1	22.2	24	24.1	25	25.3	26.1
	Pole2	22.1	22.2	25.6	26.1	26	27
	Pole3	22.2	24.1	24.3	25.2	26	26.5
Type-II (semi-elliptic air duct)	Pole1	24.6	24.2	26.1	26.9	27.2	27.5
	Pole2	24.6	25.3	25.8	26.2	27.1	27.3
	Pole3	24.6	26.5	26.6	27	27.4	28

Table 5 Experimental results obtained by adopting IJV System, case-II (0.1h)

Type of supply air duct	Pole No.	Thermocouple height from the foot level(m)					
		0	0.4	0.8	1.1	1.4	1.8
		Air temperature (^{o}C)					
Type-I (square air duct)	Pole1	23.5	23.4	24.6	25.3	26.1	26.3
	Pole2	23.5	24.2	24.9	25.1	25.7	26.2
	Pole3	23.5	24.1	25.5	25.6	26.1	26.3
Type-II (semi-elliptic air duct)	Pole1	24.5	23.7	26.1	27.1	28.5	28.9
	Pole2	24.5	24.7	25.5	27.5	28.6	29.6
	Pole3	24.5	25.5	26.2	27.3	27.9	28.1

5- Results and Discussion

The simulated results for using an impinging jet ventilation system with a different cross sectional area of supply air duct are compared with experimental readings at two heights of outlet air terminal from the room foot level.

For Type-I, Case-I, at pole-1. The simulated temperature distribution is compared with the experimental measurements as shown in Fig. (18).The predicted air temperatures have deviated with the experimental results, which clearly showed the difference in the temperature curves.

The mean deviation between experimental and numerical values of the three situations of occupant distribution gives good agreement about 9%.

For Type-I, case-II at pole-1. The simulated temperature distribution is compared with the experimental measurements as shown in Fig. (19).The predicted air temperatures have deviated with the experimental results, which clearly showed the difference in the temperature curves.

The mean deviation between experimental and numerical values gives acceptable agreement of 6%.

For Type-II, Case-I, at pole-1.The simulated temperature distribution is compared with the experimental measurements as shown in Fig. (20).The predicted air temperatures have deviated with the experimental results, which clearly showed the difference in the temperature curves. The mean deviation between experimental and numerical values for the three situations of occupant distribution gives good agreement of 12%.

For Type-II, case-II at pole-1.The simulated temperature compared with the experimental measurements as shown in Fig. (21).The predicted air temperatures have deviated with the experimental results, which clearly showed the difference in the temperature curves. The percentage error between the experimental and numerical results reach 13%.

Figs. (22) to (27) display numerically the contours of air temperature distribution of the three air supply types in the non-isothermal tested room. The temperature increases

from 18 ^{o}C closely at the supply air terminal and reach about 30^{o}C near the human body and (pc) simulator. The cold air expands through the ground of the room and then passes vertically as a hot air due to heat exchange with heat sources in the room (occupants & computers). Thermal plumes are generated by convection due to the differences in temperature between the heat sources and the surrounding air. And found that the ground area near the distribution area of the display will show the lowest temperatures, due to the cooling effect of the supply enters the air. In addition, a gradual increase in temperature gained with increased height within the room.

Also, a rise in indoor temperature can be observed near the person, PC-simulator and lighting, and note the emergence of the three areas. The area of an impinging jet is generally divided into three distinct zones: the free jet area, the impingement zone and the jet-wall area, the production of excessive motor energy in the recessive zone and their distribution in longitudinal side directions on the ground.

The CFD results are plotted. Supply air with uniform velocity profile indicates the wider jet velocity distribution, especially near the outlet. After reaching the floor, the velocity with uniform velocity profile sustains longer and dissipates slower than that of a terminal outlet with boundary layer profile, this method is based on the principle of supplying a jet of air with high momentum down to the ground. As the jet impinges on the ground spreads over a wide area causing the momentum of the jet momentum, but still has enough power to reach long distances.

Figs. (28) to (33) present streamlines flow patterns for all different types of air IJV supply ducts and at two outlet heights (0.1h, 0.14h). Beneath the ceiling, air moves in a general tendency towards the air inlet wall, driven by buoyancy forces from the thermal plume. Due to buoyancy effects from internal heat sources (e.g. occupant), the flow tends to be directed towards the opposite side of the room. Close to the corner between the inlet and rear walls. This downward flow merges with primary flows in the lower part of the room and consequently increases the momentum of the flow penetrating into the room, which leads to a higher velocity at certain positions as well as a longer flow projection to the room.

Acceptable Air Distribution Performance Index (ADPI), effective temperature, and ventilation efficiency are determined as illustrated in table 6. The square cross sectional supply area of supply air duct at 0.1h height from foot level gives acceptable agreement than other types. Also a good air distribution system not only promotes a comfortable and healthy environment for occupants, but also contributes to energy conservation.

6- **Conclusions**

The present work focuses on the analysis and design of air quality and human thermal comfort in rooms by comparing three cross sectional types of supply air duct adopting impinging jet ventilation system at different heights from foot level under Iraqi climate.

The following conclusions can be summarized from the results of the present study:

1- Assessment of three cross sectional area of supply air duct in impinging jet ventilation system obtained that the square air supply device has been found to reduce the overall discomfort than semi-elliptic and rectangle shapes. And gives more acceptable agreement than other types. Also present good air distribution system not only promotes a comfortable and healthy environment for occupants, but also contributes to energy conservation, gives a more nearest to the standard Iraqi Cooling code in a theoretical analysis study for office room.
2- Optimum Air Distribution Performance Index (ADPI), effective temperature, and ventilation efficiency was found from the square cross sectional area of supply air duct are when compared with the other types in terms of human thermal comfort and indoor air quality.

Table 6 Numerical values of ADPI, effectiveness temperature

Supply duct type	Type-I		Type-II		Type-III	
Distance from the foot level	Case-I	Case-II	Case-I	Case-II	Case-I	Case-II
ADPI%	0.76	0.77	0.73	0.63	0.40	0.64
Effectiveness	1.13	1.59	0.93	0.90	0.59	0.65

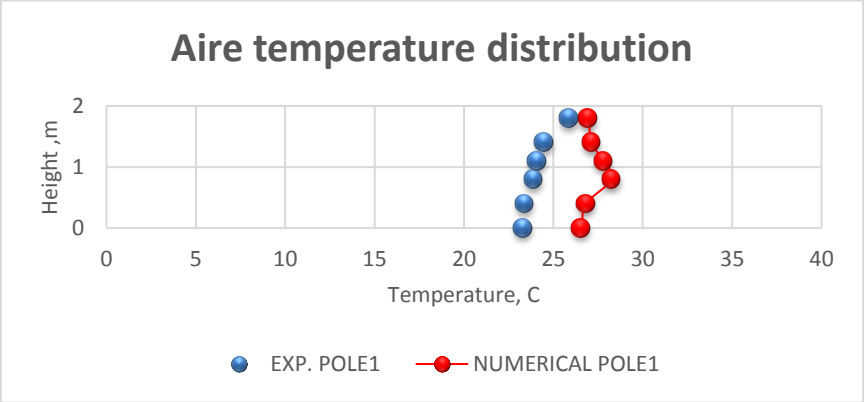

Fig. 18. Comparison between predicted and experimental results, Type-I, case-I

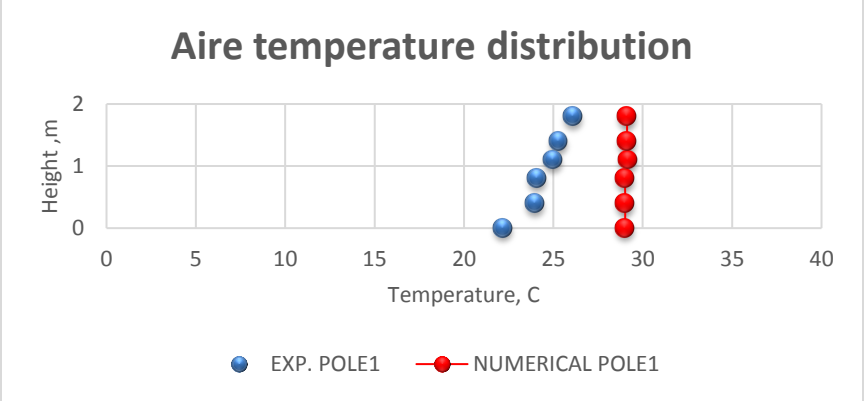

Fig. 19. Comparison between predicted and experimental results, Type-I, case-II

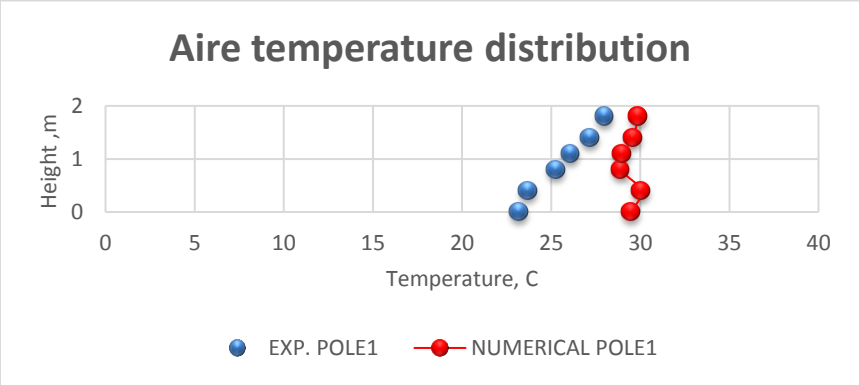

Fig. 20. Comparison between predicted and experimental results, Type-II, case-I

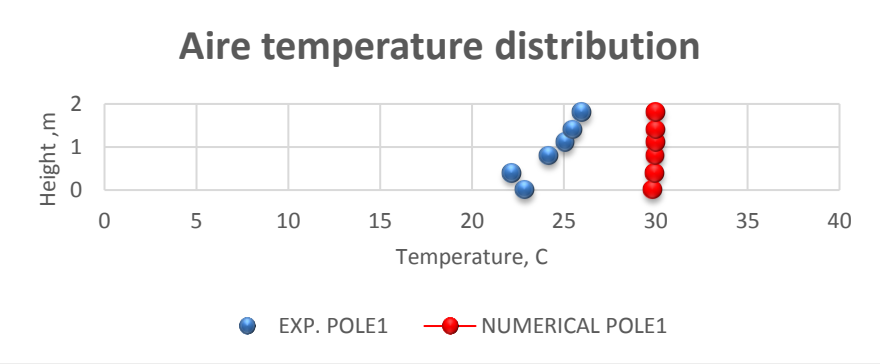

Fig. 21. Comparison between predicted and experimental results, Type-II, case-II

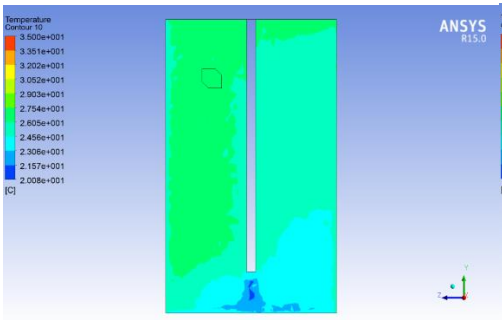

Fig. 22. Temperature contour at plane-4 for the impinging jet ventilation, Type-I, case-I

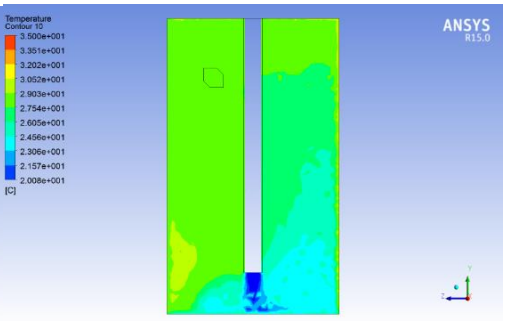

Fig. 23. Temperature contour at plane-4 for the impinging jet ventilation, Type-II, case-I

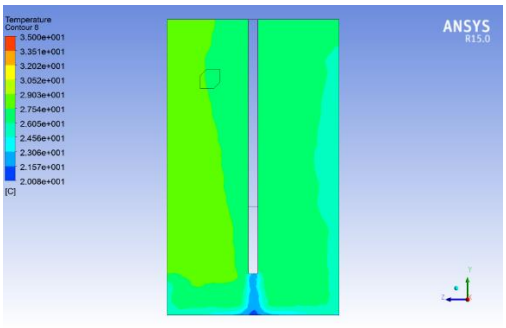

Fig. 24. Temperature contour at plane-4 for the impinging jet ventilation, Type-III, case-I

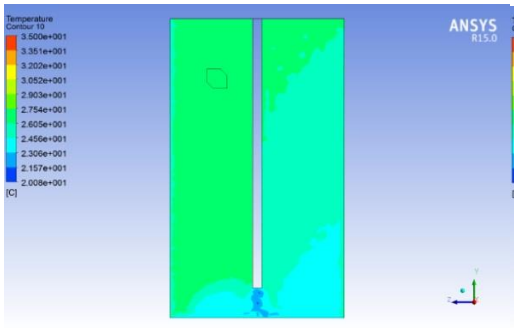

Fig. 25. Temperature contour at plane-4 for impinging jet ventilation, Type-I, case-II

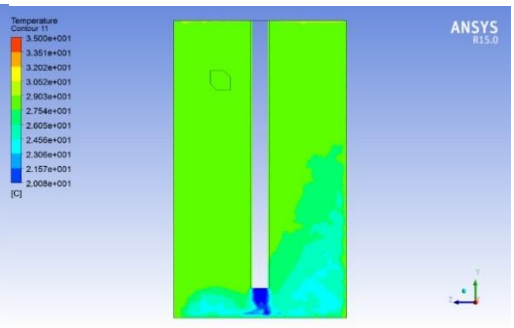

Fig. 26. Temperature contour at plane-4 forthe the impinging jet ventilation, Type-II, case-II

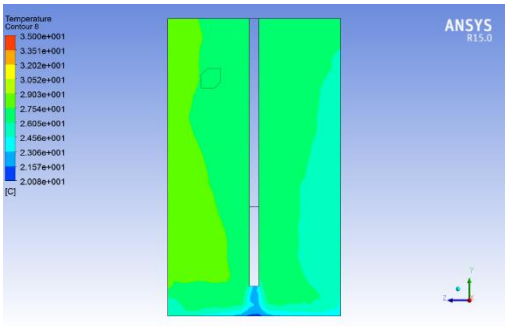

Fig. 27. Temperature contour at plane-4 for the impinging jet ventilation, Type-III, case-II

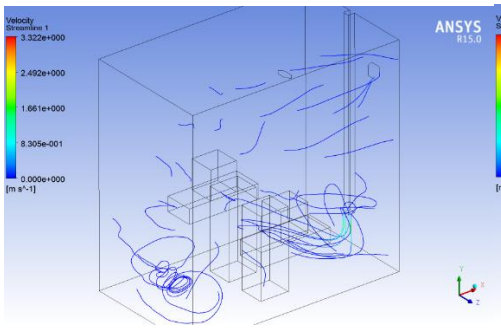

Fig. 28. The computed streamlines for IJV perspective view, Type-I, case-I

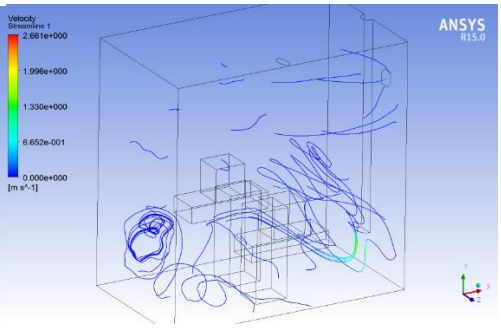

Fig. 29. The computed streamlines for IJV perspective view, Type-II, case-I

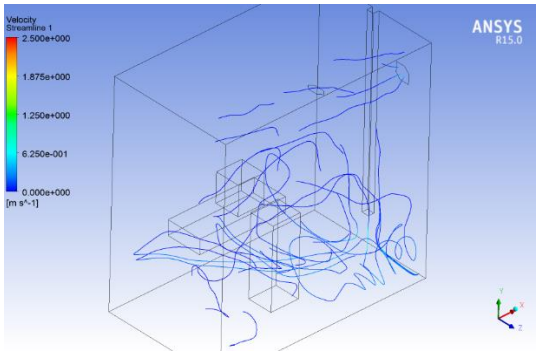

Fig. 30. The computed streamlines for IJV perspective view, Type-III, case-I

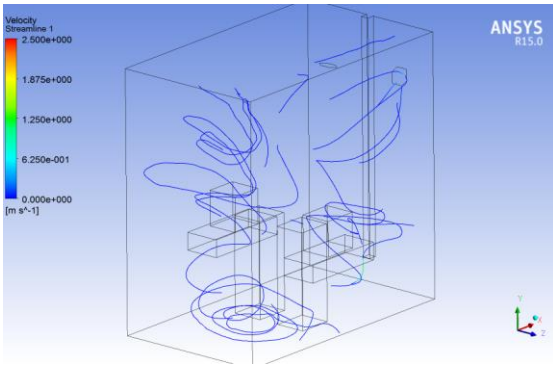

Fig. 31. The computed streamlines for IJV perspective view, Type-I, case-II

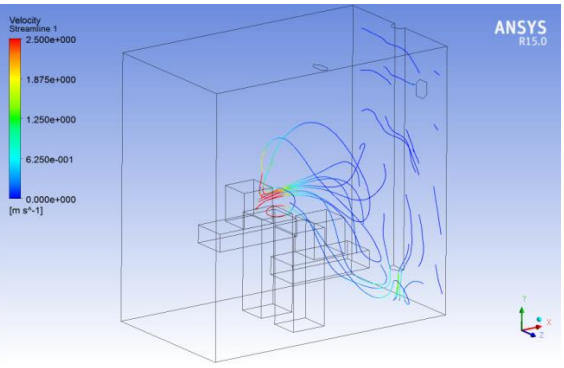

Fig.32. The computed streamlines for IJV perspective view, Type-II, case-II

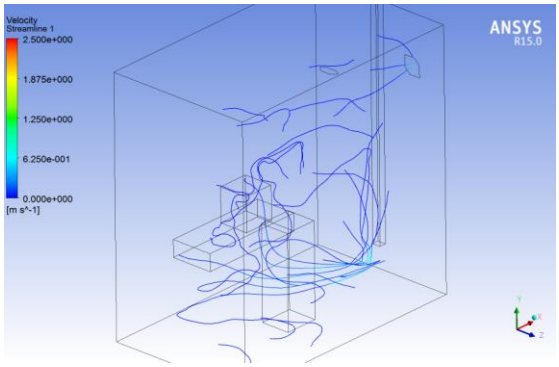

Fig.33. The computed streamlines for IJV perspective view, Type-III, case-II

7- References

ASHRAE. Standard 55-2004, 2004,"Thermal environmental conditions for human occupancy". Atlanta, GA: American Society for Heating, Refrigerating and Air Conditioning Engineers.

Awbi H. B., 2003, "Ventilation of Buildings", Spon Press, second edition.

Chen Q. & Glicksman L., ,2003 ,"System performance evaluation and design guidelines for displacement ventilation". Atlanta, GA: American Society of Heating, Refrigerating, and Air-conditioning Engineers, Inc.

Chen HJ, Moshfegh B, Cehlin M. Investigation on the flow and thermal behavior of impinging jet ventilation systems in an office with different heat loads. Building and Environment;59:127e44.

Chen HJ, Moshfegh B, Cehlin M., 2012, Numerical investigation of the flow behavior of an isothermal impinging jet in a room. Building and Environment;49:154e66.

Chen Q. & Glicksman L. ,2003, "System performance evaluation and design guidelines for displacement ventilation". Atlanta, GA: American Society of Heating, Refrigerating, and Air-conditioning Engineers, Inc.

Huijuan Chen , 2014, "Experimental and numerical investigations of a ventilation strategy – impinging jet ventilation for an, office environment", Msc.thesis, Linköping University.

Karimipanah T, Awbi HB. ,2002,Theoretical and experimental investigation of impinging jet ventilation and comparison with wall displacement ventilation.Building and Environment;37:1329e42.

Karimipanah T, Sandberg M, Awbi HB, 2013, A comparative study of different air distribution systems in a classroom. Reading, UK. In: Proceedings of 7th international conference on air distribution in rooms 2000. p. 1013e8.

Karimipanah[a] T., Awbi[b,*] H.B. , 2001, "Theoretical and experimental investigation of impinging jet ventilation and comparison with wall displacement ventilation", The University of Reading,reading RG6 6AW, UK.

Lee K, Xue GQ, JIANG Z, Chen QY, 2012. Thermal environment in indoor spaces with under-floor air distribution systems: 1. Impact of design parameters. HVAC&R Research;18(6):1182e91.

Rohdin P, Moshfegh B. ,2007, Numerical predictions of indoor climate in large industrial premises. A comparison between different kεε models supported by field measurements. Building and Environment;42:3872e82.

Varodompun J, Navvab M., 2007, HVAC ventilation strategies: the contribution for thermal comfort, energy efficiency, and indoor air quality. Journal of Green Building;2(2):131e50.

Varodoumpun J, Navvab M., 2007, The impact of terminal configuration in impinging jet ventilation room. Sendai, Japan. In: The 6th international conference on indoor air quality, ventilation & energy conservation in buildings IAQVEC.